

Exciton splitting and carrier transport across the amorphous-silicon/polymer solar cell interface

Vignesh Gowrishankar,^{a)} Shawn R. Scully, and Michael D. McGehee^{b)}

Department of Materials Science and Engineering, Stanford University, Stanford, California 94305

Qi Wang and Howard M. Branz

National Renewable Energy Laboratory (NREL), 1617 Cole Blvd., Golden, Colorado 80401

(Received 24 April 2006; accepted 15 November 2006; published online 18 December 2006)

The authors study exciton splitting at the interface of bilayer hybrid solar cells to better understand the physics controlling organic-inorganic device performance. Hydrogenated amorphous silicon (*a*-Si:H)/poly(3-hexylthiophene) (P3HT) and *a*-Si:H/poly(2-methoxy-5-(2'-ethyl-hexyloxy)-1,4-phenylenevinylene) (MEH-PPV) solar cells show photoresponse dominated by exciton production in the polymer. The *a*-Si:H/P3HT devices are nearly as efficient as titania/P3HT cells. However, the *a*-Si:H/MEH-PPV system has much lower photocurrent than *a*-Si:H/P3HT, likely due to inefficient hole transfer back to the MEH-PPV after energy transfer from MEH-PPV to *a*-Si:H. © 2006 American Institute of Physics. [DOI: 10.1063/1.2408641]

Hybrid organic-inorganic solar cells combine the processability and strong complementary absorption of organic semiconductors with the higher charge carrier mobilities of inorganic semiconductors. Nanostructured hybrids can be made by filling nanoporous inorganic films with the organic semiconductor. In the past, various hybrid cells of inorganic/organic pairs have been reported, including GaAs with thiophene derivatives,¹ nanorod CdSe with polythiophene,² Si with polyacetylene³ and Cu-phthalocyanine,⁴ and titania with conjugated polymers.⁵⁻⁷ In this work, we use hydrogenated amorphous silicon (*a*-Si:H) as the inorganic material because it is an inexpensive deposited semiconductor that is much cheaper and easier to pattern than GaAs, enables the creation of rigid, well-controlled nanostructures,^{8,9} and absorbs more strongly than crystalline Si or titania. Among *a*-Si:H/polymer solar cells, previous work¹⁰ reported cells having light absorption primarily in the *a*-Si:H, whereas our work is the first to report on cells having most of the light absorption in the polymer. We report on the fabrication and photovoltaic properties of *a*-Si:H/poly-(3-hexylthiophene) (P3HT) and *a*-Si:H/poly(2-methoxy-5-(2'-ethyl-hexyloxy)-1,4-phenylenevinylene) (MEH-PPV) bilayer solar cells. Current-voltage characteristics of these cells are compared with titania/P3HT and titania/MEH-PPV bilayer cells in Fig. 1. We find that the *a*-Si:H/P3HT devices are almost as efficient as the titania/P3HT devices. However, the *a*-Si:H/MEH-PPV devices exhibit much lower efficiency than either the *a*-Si:H/P3HT or the titania/MEH-PPV devices. We attribute the greatly reduced efficiency of *a*-Si:H/MEH-PPV to a combination of the low MEH-PPV highest occupied molecular orbital (HOMO) level (high ionization potential) and the extended valence bandtail states in the *a*-Si:H.

All four systems of P3HT and MEH-PPV on *a*-Si:H and titania were bilayer devices. The 100-nm-thick films of titania, on fluorine doped tin oxide-coated glass (bottom electrode), were prepared using a sol-gel route as reported previously.¹¹ About 20 nm of *a*-Si:H was deposited on flat indium tin oxide-coated glass (bottom electrode) using the

hot-wire chemical vapor deposition technique.¹² The *a*-Si:H surface was treated with dilute hydrofluoric acid to remove the native oxide. All subsequent steps were performed in a nitrogen atmosphere inside a glove box. The 60-nm-thick P3HT and MEH-PPV films were spin coated onto the inorganic substrates from suitably concentrated solutions in tetrahydrofuran. The *a*-Si:H and polymer thicknesses were just sufficient to prevent shorting; thicker *a*-Si:H was avoided to enable maximum absorption in the polymer (*vide infra*). Due to low exciton diffusion lengths (under 10 nm¹³), larger polymer thicknesses do not increase efficiencies. Then, 70 nm of Ag was evaporated onto the polymer layer to form the top electrode. The completed devices were annealed at 135 °C for 3–10 h to obtain optimal photovoltaic performance, as determined with a Spectra-Physics 81150 solar simulator operated at AM 1.5 conditions.

Titania is transparent in the visible region of the solar spectrum, whereas *a*-Si:H is strongly absorbing in this region. Under illumination, the electron-hole pairs created in the polymer are excitonic in nature, whereas electron-hole pairs in the *a*-Si:H are probably unbound due to exciton binding energies under 0.1 eV.¹⁴ As discussed below, generation in the *a*-Si:H is not a significant contributor to the photocurrent; most of the photocurrent arises from excitons generated in the polymer. These excitons could be separated and

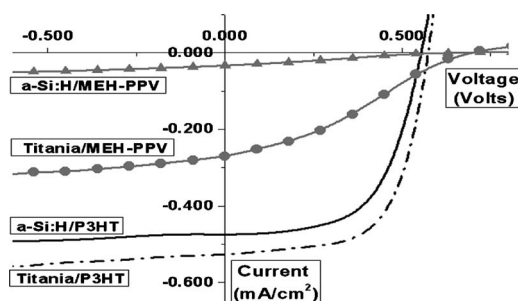


FIG. 1. Current-voltage curves of the four hybrid systems. In parentheses, short-circuit current, open-circuit voltage, fill-factor and power-conversion efficiency of titania/P3HT (broken: 0.53 mA/cm², 585 mV, 0.62, 0.19 %), *a*-Si:H/P3HT (solid: 0.47 mA/cm², 555 mV, 0.59, 0.16 %), titania/MEH-PPV (circles: 0.27 mA/cm², 685 mV, 0.31, 0.06 %) & *a*-Si:H/MEH-PPV (triangles: 0.03 mA/cm², 615 mV, 0.26, 0.01 %).

^{a)}Electronic mail: vigneshg@stanford.edu

^{b)}Electronic mail: mmcgehee@stanford.edu

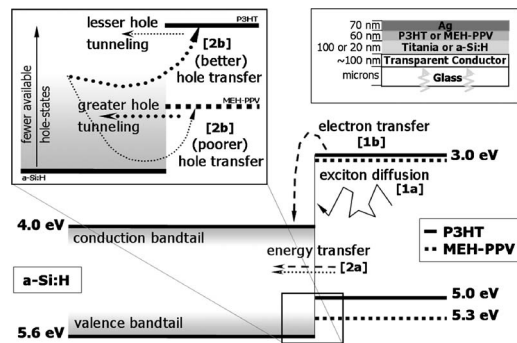


FIG. 2. (Bottom and top left) Vacuum-referenced energy levels of MEH-PPV (Ref. 7), P3HT (Ref. 16), and *a*-Si:H (Ref. 17). Titania (levels not shown) has conduction and valence band edges at ~ 4.2 eV and ~ 7.4 eV, respectively. Energy levels of *a*-Si:H are approximated from the mobility edges, but exponential tails of localized states (bandtails, in graded gray) extend into the mobility gap (Ref. 17). Two mechanisms for exciton harvesting are shown: [1a] exciton diffusion followed by [1b] electron transfer, and [2a] energy transfer (this cannot occur in titania/polymer cells) followed by [2b] hole transfer. A hole-tunneling step detrimental to exciton harvesting by mechanism [1] is also shown. See main text for details. (Top right) Schematic diagrams of the bilayer devices studied.

collected by either of the two mechanisms shown schematically in Fig. 2. In the first mechanism, exciton diffusion to the polymer-inorganic interface is followed by forward electron transfer from the polymer to the inorganic semiconductor. This mechanism is enhanced by large exciton diffusion lengths and a suitable offset between the polymer lowest unoccupied molecular orbital (LUMO) and the inorganic conduction band. In the second mechanism, Förster-like¹⁵ energy transfer occurs, wherein excitons in the donor semiconductor (polymer) are transferred to the acceptor semiconductor (inorganic),¹⁶ prior to hole transfer from the inorganic back to the polymer. In both mechanisms, the final state is an electron in the inorganic semiconductor and a hole in the polymer, and these carriers are collected at the electrodes. For energy transfer, the donor energy gap must be larger than the acceptor band gap, implying that energy transfer is possible from MEH-PPV and P3HT (energy gaps ~ 2.3 and ~ 2.0 eV, respectively^{7,16}) to *a*-Si:H (band gap ~ 1.6 eV),¹⁷ but not to titania (band gap ~ 3.2 eV).

Figure 3 shows the photocurrent-action spectra of the four hybrid systems, along with the measured polymer and *a*-Si:H absorption spectra. In the *a*-Si:H/P3HT and *a*-Si:H/MEH-PPV systems, a shoulder was clearly seen at wavelengths below approximately 450 nm, coinciding quite well with the increasing absorptivity of *a*-Si:H and clearly not attributable to the polymers' decreasing absorptivities. In the 375–450 nm wavelength range, the photocurrent contribution from *a*-Si:H in the *a*-Si:H/P3HT cell when illuminated in a solar simulator was calculated by integrating (over the range) the product of the number of photons available from the simulated solar spectrum with the external quantum efficiency at each wavelength. It was found to be only about 10% of the total photocurrent, mainly because of the low number of photons in this wavelength range. Below 375 nm, the *a*-Si:H contribution is insignificant due to a negligible number of photons. The photocurrent-action spectra of the titania/polymer systems simply tracked the absorption spectra of the polymers, with no short-wavelength shoulder, although they were somewhat broadened, possibly due to optical interference effects.¹³

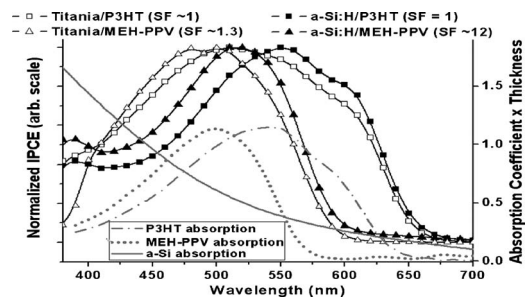


FIG. 3. Photocurrent-action spectra of normalized incident photon to charge-carrier efficiency (IPCE) vs wavelength of titania/P3HT (hollow squares), *a*-Si:H/P3HT (solid squares), titania/MEH-PPV (hollow triangles), and *a*-Si:H/MEH-PPV (solid triangles) are shown. SF denotes the scaling factors used to convert the absolute photocurrent-action spectra to normalized ones. Absorption spectra, absorption coefficient \times thickness (proportional to optical density) vs wavelength, of P3HT (dotted), MEH-PPV (dashed), and *a*-Si:H (solid) are also shown.

We first examine the performance of *a*-Si:H/P3HT and compare it with titania/P3HT. As described in more detail elsewhere,¹³ we modeled the optical properties and interference effects of the stack of materials in the devices (Fig. 2: top right). The modeling predicted about three times more generated excitons in the P3HT when on titania than when on *a*-Si:H, mainly because of the high index mismatch in *a*-Si:H/P3HT. Therefore, other parameters (e.g., exciton diffusion length, electron transfer rate) being equal and neglecting photocurrent contribution from *a*-Si:H, the modeling predicted titania/P3HT to have a short-circuit current (J_{SC}) about three times higher than *a*-Si:H/P3HT. However, J_{SC} of the two systems were roughly equal (Fig. 1) although collection from the *a*-Si:H accounts for only about 10% of the *a*-Si:H/P3HT current. The titania surface is hydrophilic, whereas the *a*-Si:H is hydrophobic; it is thus possible that the morphology of the P3HT is different on these surfaces, resulting in different exciton diffusion lengths and/or electron transfer rates. The *a*-Si:H/P3HT and titania/P3HT have similar J_{SC} , open-circuit voltage (V_{OC}) and fill factors making the *a*-Si:H/P3HT cell almost as efficient as the titania/P3HT cell. Preliminary modeling results indicated that by reducing the *a*-Si:H thickness to 10 nm, a threefold increase in the J_{SC} , and efficiency, can be expected, provided shorting problems due to pinholes can be avoided.

We analyzed the results of the four hybrid systems vis-à-vis the first mechanism of exciton harvesting, viz., exciton diffusion and electron transfer. The offsets between the polymer LUMO and the inorganic conduction band were roughly similar for all four hybrid systems (Fig. 2) and are thus not the probable cause of either of the following observations: (1) *a*-Si/MEH-PPV had a J_{SC} nine times lower than titania/MEH-PPV. Optical interference effects alone can, at most, account for only a threefold difference, nor can the difference be accounted for by dissimilar electronic properties of MEH-PPV on the different inorganic semiconductors: because it is amorphous, MEH-PPV is expected to have similar exciton diffusion lengths on and electronic interaction with each inorganic semiconductor. (2) Though titania/MEH-PPV has a J_{SC} only two times lower than titania/P3HT (probably due to differences in exciton diffusion lengths and/or electron transfer efficiencies), *a*-Si:H/MEH-PPV has a J_{SC} 16 times lower than *a*-Si:H/P3HT. This difference is far greater than the twofold difference seen with the polymers on titania. Also, this 16-fold difference cannot be due to low hole mo-

bility in MEH-PPV because nine times as much current flux (mA/cm^2) can pass through the same thickness of MEH-PPV when on titania. Thus, *a*-Si:H/MEH-PPV contributes much lower photocurrent than expected, and these results are inadequately explained simply by a mechanism of exciton diffusion and electron transfer.

For reasons described below, the second mechanism of exciton harvesting, energy transfer from the polymer to *a*-Si:H followed by hole transfer back to the polymer, occurring independently of and along with the first mechanism, adequately explains the results. Using a framework based on Förster energy transfer,¹⁵ it is seen that energy transfer depends, among other factors, on the photoluminescence efficiency (Q_D) of the donor (polymer). Depending on the batch of MEH-PPV used, its Q_D is between 0.10 and 0.15,¹⁸ whereas Q_D of P3HT is 0.02.¹⁸ Uncertainties in other parameters involved in the Förster framework, such as the refractive index, rendered us unable to calculate a definitive rate and probability of energy transfer in the *a*-Si:H/polymer systems. MEH-PPV, by virtue of its higher Q_D , is expected to exhibit stronger Förster-like energy transfer to *a*-Si:H than is P3HT. Excitons can thus be transferred from MEH-PPV to *a*-Si:H (where they become unbound), and to a far lesser extent from P3HT to *a*-Si:H. The holes in the *a*-Si:H need then to jump back to the polymer HOMO for collection. The schematic diagram shown in Fig. 2 (top left) suggests that hole transfer from *a*-Si:H to P3HT will have a much faster rate than from *a*-Si:H to MEH-PPV. This is consistent with the absolute photocurrent-action spectra of *a*-Si:H/P3HT and *a*-Si:H/MEH-PPV (Fig. 3); *a*-Si:H contributes eight times lower current with MEH-PPV than with P3HT. The *a*-Si:H has an exponential bandtail of localized states extending into the band gap from the valence band edge, which can trap injected or photoexcited holes. Under 1 sun illumination there is significant hole occupation only above the hole quasi-Fermi level, which is about 0.5 eV above the *a*-Si:H valence band edge.¹⁹ To cross from *a*-Si:H to the polymer, these holes deep in the valence bandtail need to jump to the polymer HOMO. The number of bandtail holes for which a jump to the HOMO is energetically favorable depends on the HOMO level. The reported vacuum-referenced HOMO values for MEH-PPV and P3HT are ~ 5.3 eV (Ref. 7) and ~ 5.0 eV,¹⁶ respectively. These values are also supported by the larger observed V_{OC} in *a*-Si:H/MEH-PPV than in *a*-Si:H/P3HT. Since the MEH-PPV HOMO is closer to the *a*-Si:H valence band edge than is the P3HT HOMO, hole transfer from *a*-Si:H to MEH-PPV is far slower than to P3HT. Stronger energy transfer from MEH-PPV (than from P3HT) to *a*-Si:H, followed by poorer hole transfer back to MEH-PPV (than to P3HT) thus predicts lower J_{SC} in *a*-Si:H/MEH-PPV, as was observed. Alternatively, the mechanism of exciton diffusion followed by electron transfer could also explain the low *a*-Si:H/MEH-PPV J_{SC} , but only if we include the possibility of deleterious hole tunneling from the polymer to the *a*-Si:H (Fig. 2). With the HOMO levels and *a*-Si:H bandtail hole occupation as described above, it is easier for holes to tunnel into electron-occupied *a*-Si:H valence bandtail states from MEH-PPV than from P3HT. The tunneling rate may be increased by the Coulombic attraction from trapped electrons in the *a*-Si:H, near the interface (after electron transfer from

the polymer). Thus greater hole tunneling, likely in conjunction with stronger energy transfer, to *a*-Si:H from MEH-PPV (than from P3HT), together with poorer hole transfer back to MEH-PPV (than to P3HT), could also explain the lower J_{SC} in *a*-Si:H/MEH-PPV.

In conclusion, we have demonstrated that the *a*-Si:H/P3HT bilayer devices are almost as efficient as the titania/P3HT devices, while the *a*-Si:H/MEH-PPV system exhibits much lower efficiency. The use of *a*-Si:H with P3HT offers the possibility of significant efficiency improvements via nanostructuring of the *a*-Si:H. In general, when considering suitability of an organic/inorganic pair of materials for heterojunction solar cells, if exciton diffusion and forward electron transfer is dominant, conduction band (LUMO) offset will be critical, but the valence band (HOMO) offset must also be suitable. If energy transfer is strong and dominant, then backward hole transfer efficiency, controlled by the valence band (HOMO) offset, will be the most important factor. The relative positions of the polymer HOMO and the hole quasi-Fermi level in the *a*-Si:H thus play a key role in determining the critical hole transfer rates.

Three of the authors (V.G., S.R.S., and M.D.M.) thank Robert Street and Jackson Ho of Palo Alto Research Center for *a*-Si:H samples used in the early stages of the work. They also acknowledge the U.S. Department of Energy (DOE) and Global Climate and Energy Project for funding. Work at NREL was supported by the U.S. DOE under Contract No. DE-AC36-99GO10337.

¹F. Garnier, *J. Opt. A, Pure Appl. Opt.* **4**, S247 (2002).

²W. U. Huynh, J. J. Dittmer, and A. P. Alivisatos, *Science* **295**, 2425 (2002).

³M. J. Sailor, E. J. Ginsburg, C. B. Gorman, A. Kumar, R. H. Grubbs, and N. S. Lewis, *Science* **249**, 1146 (1990).

⁴I. A. Levitsky, W. B. Euler, N. Tokranova, B. Xu, and J. Castracane, *Appl. Phys. Lett.* **85**, 6245 (2004).

⁵K. M. Coakley and M. D. McGehee, *Appl. Phys. Lett.* **83**, 3380 (2003).

⁶C. Y. Kwong, A. B. Djurisic, P. C. Chui, K. W. Cheng, and W. K. Chan, *Chem. Phys. Lett.* **384**, 372 (2004).

⁷A. J. Breeze, Z. Schlesinger, S. A. Carter, and P. J. Brock, *Phys. Rev. B* **64**, 125205 (2001).

⁸V. Gowrishankar, N. Miller, M. D. McGehee, M. J. Misner, D. Y. Ryu, T. P. Russell, E. Drockenmuller, and C. J. Hawker, *Thin Solid Films* **513**, 289 (2006).

⁹K. W. Guarini, C. T. Black, Y. Zhang, H. Kim, E. M. Sikorski, and I. V. Babich, *J. Vac. Sci. Technol. B* **20**, 2788 (2002).

¹⁰E. L. Williams, G. E. Jabbour, Q. Wang, S. E. Shaheen, D. S. Ginley, and E. A. Schiff, *Appl. Phys. Lett.* **87**, 223504 (2005).

¹¹Y. X. Liu, S. R. Scully, M. D. McGehee, J. S. Liu, C. K. Luscombe, J. M. J. Frechet, S. E. Shaheen, and D. S. Ginley, *J. Phys. Chem. B* **110**, 3257 (2006).

¹²Q. Wang, E. Iwaniczko, Y. Xu, W. Gao, B. P. Nelson, A. H. Mahan, R. S. Crandall, and H. M. Branz, *Mater. Res. Soc. Symp. Proc.* **609**, A431 (2000).

¹³S. R. Scully and M. D. McGehee, *J. Appl. Phys.* **100**, 034907 (2006).

¹⁴R. A. Street, in *Hydrogenated Amorphous Silicon*, edited by J. I. Pankove (Academic, London, 1984), Vol. B, pp. 203–207.

¹⁵T. Förster, *Discuss. Faraday Soc.* **27**, 7 (1959).

¹⁶Y. X. Liu, M. A. Summers, C. Edder, J. M. J. Frechet, and M. D. McGehee, *Adv. Mater. (Weinheim, Ger.)* **17**, 2960 (2005).

¹⁷R. A. Street, *Hydrogenated Amorphous Silicon*, 1st ed. (Cambridge University Press, Cambridge, 1991), pp. 62–94 and 237–242.

¹⁸N. C. Greenham, I. D. W. Samuel, G. R. Hayes, R. T. Phillips, Y. A. R. R. Kessener, S. C. Moratti, A. B. Holmes, and R. H. Friend, *Chem. Phys. Lett.* **241**, 89 (1995).

¹⁹E. A. Schiff, *Sol. Energy Mater. Sol. Cells* **78**, 567 (2003).